Improvement of efficiency in CZTSSe solar cell by using back surface field

Atul Kumar, Ajay D Thakur

Department of Physics, Indian Institute of Technology Patna,
Bihta 801118, India.

E-mail: atul.pph14@iitp.ac.in

Abstract. A kesterite CZTS based solar cell is studied with back surface field. In order to achieve this, a p^+ layer of SnS is added to the standard cell configuration. The resulting p^+-p-n configuration of SnS/CZTS/CdS is studied using Solar Cell Capacitance Simulator (SCAPS). Low V_{oc} is responsible for lower efficiencies of kesterite solar cells. The proposed p^+-p-n structure increases the V_{oc} and thus the efficiency. Simulation of CZTSSe and CZTS with back surface p^+ layer has shown considerably higher efficiency than the highest reported value for kesterite cell of CZTSSe from 12.3% to 15.7%. A comparative summary is presented with literature reported performance and our simulated performance for kesterite cell.

1. Introduction

Solar cells based on $Cu_2ZnSnS_{4-x}Se_x$ (CZTSSe) can have Shockley Quisser limit of 32% as per their bandgap, and is a potential low cost photovoltaic (PV) material. The reported highest efficiency of 12.6% for kesterite CZTSSe based solar cells [1] is much less than SQ limit and chalcopyrite $CuIn_xGa_{1-x}S_2$ (CIGS) counterpart (21.6% for) [2]. This inferiority in performance of kesterite suggests complex defect physics resulting in Lower V_{oc} and overall performance [3,4]. Secondary phase and point defect in absorber layer, non optimized interfaces [3] and possible flaws in cell structure are issues which require careful attention for kesterite solar cells. For optimization of cell structure simulation tools can be utilized where cell structures/configuration, interface and their performance can be optimized. A simulation, studying the effect of various parameters on photovoltaic performance is an easy step to predict optimized conditions without actually fabricating a solar cell. AMPS, PC1D, SILVACO, SCAPS [5,6] are some extensively used solar cell simulation software. SCAPS-1D simulation software is used in this study, which solve Poisson equation, relating the charge to the electrostatic potential (φ) and Continuity equation for electrons (n_i) and holes (p_i) for simulation of devices. In one dimension, the cell is divided into N intervals and solved for (φ, n_i, p_i) at each interval. The SCAPS can simulate $CuInSe_2$, CdTe, c-Si a-Si [7], CZTSSe [6, 8] and perovskite [9]. The present work focuses on the role of back surface field. The back surface field has been reported for enhanced PV performance in a variety of solar cells [10,11]. A high-low junction p^+-p at back cause conducive band banding, an electric field in direction of p-n junction is setup decreasing electrons current at back contact. H. Cui *et al* [12] reported the increase in efficiency by adding a back surface layer in CZTSSe. In this regard we propose an SnS back surface layer to modify the overall cell structure. Cell configuration of p^+(SnS)/p(CZTSSe)/CdS/ZnO is simulated with SCAPS-1D software to study and optimize overall performance. A comparative study of p-n junction and p^+-p-n junction is presented in following section.

2. Solar cell description with back surface field

A p-n junction based photovoltaic device has built in voltage at the junction is given by

$$V = \frac{KT}{q} \ln \frac{N_a N_d}{n_i^2}$$

When a p^+ layer (layer with higher hole density) is added at back, a p^+-p high low junction is formed giving rise to a built-in voltage

$$V = \frac{KT}{q} \ln \frac{N_{a+}}{N_a}$$

Where Na, Na^+, is the hole density in the p, p^+, N_d is electron density in n layer respectively.
For a p^+-p junction, by virtue of acceptor concentration variations, band bending occurs at junction and an electric field in direction of p-n junction is set up. The generated voltage at the p^+-p junction produces a barrier for electron current at rear contact. Such high-low junction can be employed in solar cell structure at appropriate locations to induce directional flow of charge carriers in solar cell for selective contacts. This arrangement can provide higher V_{oc} and less recombination at junction and bulk. A higher V_{oc} is observed in case of an applied p^+-p in solar cell as discussed in the next section.

3. Simulation Details

A p-type SnS is used as a back surface layer. The configuration of standard cell is Mo/CZTSe/CdS/ZnO and of that for the modified cell is Mo/SnS/CZTSe/CdS/ZnO as shown in Fig. 1. A comparative study of the two cell configurations is performed using SCAPS-1D [7]. SnS is used since it has similar material composition as CZTS, suitable p-type nature and easily synthesized by various methods [13]. The material parameters used are listed in the Table I [5,8]. The device is illuminated from window layer (ZnO) side with AM1.5 spectrum using relevant SCAPS option at temperature 300 K. For the series resistance (R_s) and shunt resistance (R_{sh}), we have used typical values of 0.72 ohm-cm^2 and 620 ohm-cm^2, respectively which are conservative estimates considering the experimentally reported values of 0.72 ohm-cm^2 and 620 ohm-cm^2, respectively [1].The Schematic of the two configuration is shown in the Fig.1.

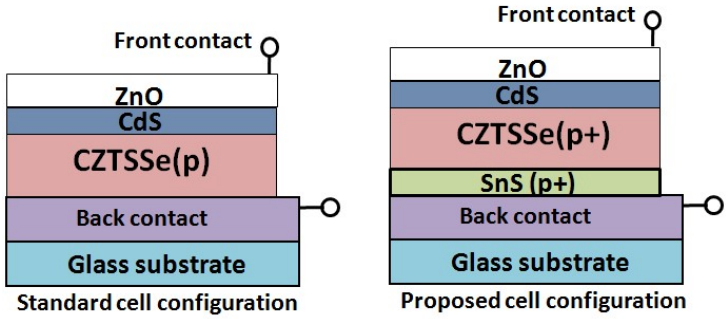

Figure 1: Schematic diagram of the conventional cell configuration and the proposed cell configuration for CZTSSe based solar cells.

Table 1. Material parameters used in simulations [6,7,14].

Parameters	**SnS**	***CZTSSe***	**CdS**	***ZnO***
Thickness(nm)	100	2000	80	200
Bandgap(eV)	1.25	1.3	2.4	3.3
Electron affinity	3.9	4.2	4.5	4.6
Dielectric permittivity	13.7	13	10	9
Electron/hole mobility(cm^2/Vs)	30/15	100/25	350/50	100/25
Donor/acceptor density(cm^{-3})	$10/10^{18}$	$10/10^{15}$	$10^{17}/10$	$10^{18}/10$

4. Results and Discussion

4.1. Absorber layer: CZTSSe

The quality of interface between the CZTSSe absorber layer and the CdS buffer layer is crucial in the separation of generated electron-hole pairs. The recombination in bulk leading to losses is primarily caused by radiative processes, non-radiative (Shockley-Read-Hall mechanism) processes, and the interface recombination which increases saturation current and thus decreases V_{oc}. In case of polycrystaline absorber, inhomogeneities in band gap variations and electrostatic fluctuations increases the saturation current. Here, CZTSSe passivated with SnS is observed to have a better performance as shown in Fig. 2. The gain in performance is seen along with higher V_{oc}, fill factor (FF) and J_{sc} in cell with SnS. Typical thicknesses for SnS and CdS were chosen as 100 nm and 80 nm, respectively. The p^{+}-p and the p-n junctions at either side of absorber layer creates an asymmetry for charge flow. The efficiency with the thickness of the absorber layer is shown in Fig.2. The V_{oc} for the SnS/CZTSSe/CdS/ZnO configuration is observed to be higher than the unpassivated cell due to the generation of the built-in voltage at both the ends of the absorber layer. Short circuit current, I_{sc} of the passivated cell is higher than the unpassivated counterpart due to the presence of a directed field for charge flow in absorber layer.

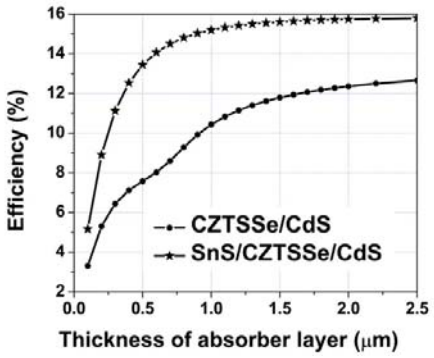

Figure 2: Variation of efficiency with absorber layer thickness in the investigated cell configurations.

4.2. Band-diagram for CZTS solar cell.

Simulated band diagram shown in Fig. 3 convey band bending at junction/interfaces and energy levels in bulk. The Fermi level splitting at p-n junction gives rise to a light induced voltage. The addition of SnS back surface layer leads to the formation of a high-low junction by virtue of difference in acceptor concentration in SnS and CZTSSe. The higher energy level of SnS than CZTSe in band diagram in Fig. 3 is a favorable condition as an electric field is set up at both ends of the absorber layer. Generated charge carrier in absorber will feel a drift field thereby increasing its probability of collection at junction. A high low junction at the rear also acts as the near ohmic contact.

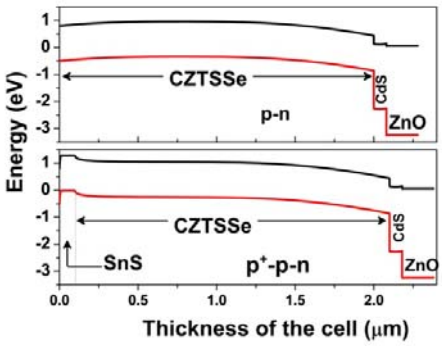

Figure 3: Simulated band diagram for the two configuration of cells.

4.3. Quantum efficiency.

Quantum efficiency shows the charge pair generated by absorption of different wavelength. Different wavelengths are absorbed at different thickness. Higher wavelengths are absorbed in deeper in bulk of absorber and low wavelength light is absorbed at surface. The band gap of CZTSSe (1.3eV) corresponds to 954nm wavelength. The QE is observed to improve at higher wavelength i.e. in depth at rear side in the modified cell configuration. This is due to SnS back surface field which efficiently created at field thus efficient collection of charge carriers.

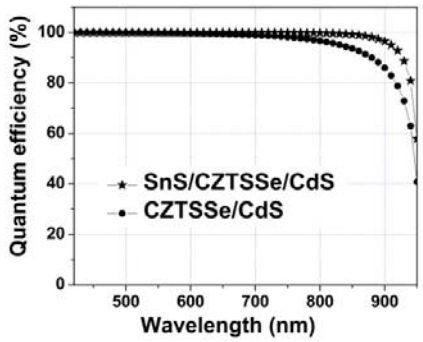

Figure 4: Quantum efficiency measurements for the solar cell configurations under investigation.

5. Conclusions

The back surface field in CZTSSe can improve V_{oc} in cell by creating a built in voltage at rear, It also improve the contact of metal semiconductor making a near ohmic metal-p^+-p. In our work we simulated back surface using an SnS layer and showed that a structure of p^+-p-n is useful for solar cell performance improvement. A higher V_{oc} is obtained in CZTSSe cell along with improved FF and QE. We have increased the efficiency of cell from 12.3 to 15.7% by incorporation of back surface field. The comparative performance of all the simulated and experimentally reported cell of CZTSSe cell is shown in Fig. 5 and tabulated in Table 2.

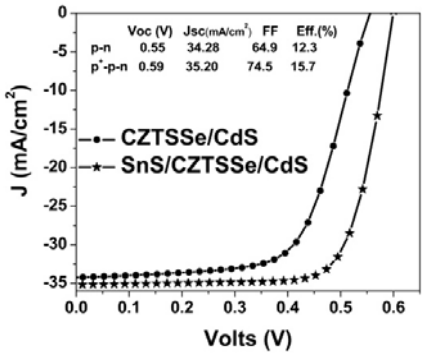

Figure 5: I-V curve of the two cell configuration and the simulated parameters.

Table 2. Comparative performance of different configuration.

Configuration	V_{oc} (V)	J_{sc} *(mA/cm²)*	FF (%)	η (%)	Reference
CZTSe/CdS/ZnO	0.513	35.2	69.8	12.6	[1]
CZTSe/CdS/ZnO	0.55	34.28	64.9	12.3	Our simulation
SnS/ CZTSe/CdS/ZnO	0.59	35.20	74.5	15.7	Our simulation

Acknowledgments
The solar cell capacitance simulator SCAPS-1D used here is generously provided by Dr. Marc Burgelman from the University of Gent.

References

[1] Wang W, Winkler M T, Gunawan O, Gokmen T, Todorov T K, Zhu, Y., Mitzi D B 2014. Device Characteristics of CZTSSe Thin-Film Solar Cells with 12.6% Efficiency, *Adv. Energy Mater* **4** 1301465.
[2] Jackson P, Hariskos D, Wuerz R, Kiowski O, Bauer A, Friedlmeier T M and Powalla M, 2015 Properties of Cu(In,Ga)Se_2 solar cells with new record efficiencies up to 21.7% *Phy. Status Solidi RRL* **9** 28–31
[3] Polizzotti A, Repins I L, Noufi R, We, Su-Huai and Mitzi DB, 2013 The state and future prospects of kesterite photovoltaics. *Energy Environ. Sci*., **6** 3171-3182.
[4] Mark T W, Wang W, Gunawan O, Harold J. Hovel, Todorov T K and Mitzi D B, 2014 Optical designs that improve the efficiency of $Cu_2ZnSn(S,Se)_4$ solar cells, *Energy Environ. Sci*. **7** 1029.
[5] Patel M, Ray A 2012 Enhancement of output performance of Cu_2ZnSnS_4 thin film solar cells—A numerical simulation approach and comparison to experiments, *Physica B: Condensed Matter*, **407** 4391-4397.
[6] Burgelman M, Nollet P, Degrave S 2000 Modelling polycrystalline semiconductor solar cells. *Thin Solid Films* **361**, 527-532
[7] Niemegeers A, Burgelman M, Decock K, Verschraegen J, Degrave S, SCAPS Mannual, Version Date: June 27, (2015).
[8] Simya O K, Mahaboobbatcha A, Balachander K 2015 A comparative study on the performance of Kesterite based thin film solar cells using SCAPS simulation program. *Superlattices and Microstructures* **82**, 248.
[9] Minemotoa T and Murata M 2014 Device Device modeling of perovskite solar cells based on structural similarity with thin film inorganic semiconductor solar cells, *Journal of Applied Physics*, **116** 054505.

[10] Fossum J G1977 Physical operation of back-surface-field silicon solar cells *IEEE TRANSACTIONS ON ELECTRON DEVICES* **24** 4.
[11] Roos O V 1978 A simple theory of back surface field (BSF) solar cells, *Journal of Applied Physics* **49**, 3503.
[12] Cui H, Chang-Yeh Lee, Li W, Liu X, Wen X, and Hao X 2015 Improving Efficiency of Evaporated Cu_2ZnSnS_4 Thin Film Solar Cells by a Thin Ag Intermediate Layer between Absorber and Back Contact *International Journal of Photoenergy* Article ID 170507
[13] Antoine de Kergommeaux, Jérôme Faure-Vincent, Adam Pron, Rémi de Bettignies, Peter Reiss 2013 SnS thin films realized from colloidal nanocrystal inks, *Thin Solid Films*, **535** 376-379.